

12th INTERNATIONAL WORKSHOP ON RADIATION IMAGING DETECTORS,
JULY 11th–15th 2010,
ROBINSON COLLEGE, CAMBRIDGE U.K.

AMIC: an expandable integrated analog front-end for light distribution moments analysis

M. Spaggiari,¹ V. Herrero, C.W. Lerche, R. Aliaga, J.M. Monzó and R. Gadea

*Instituto de Instrumentación para Imagen Molecular (I3M), Universidad Politécnica de Valencia,
Camino de Vera, 46022, Valencia, Spain*

E-mail: michele.spaggiari@gmail.com

ABSTRACT: In this article we introduce AMIC (Analog Moments Integrated Circuit), a novel analog Application Specific Integrated Circuit (ASIC) front-end for Positron Emission Tomography (PET) applications. Its working principle is based on mathematical analysis of light distribution through moments calculation. Each moment provides useful information about light distribution, such as energy, position, depth of interaction, skewness (deformation due to border effect) etc. A current buffer delivers a copy of each input current to several processing blocks. The current preamplifier is designed in order to achieve unconditional stability under high input capacitance, thus allowing the use of both Photo-Multiplier Tubes (PMT) and Silicon Photo-Multipliers (SiPM). Each processing block implements an analog current filtering by multiplying each input current by a programmable 8-bit coefficient. The latter is implemented through a high linear MOS current divider ladder, whose high sensitivity to variations in output voltages requires the integration of an extremely stable fully differential current collector. Output currents are then summed and sent to the output stage, that provides both a buffered output current and a linear rail-to-rail voltage for further digitalization. Since computation is purely additive, the 64 input channels of AMIC do not represent a limitation in the number of the detector's outputs. Current outputs of various AMIC structures can be combined as inputs of a final AMIC, thus providing a fully expandable structure. In this version of AMIC, 8 programmable blocks for moments calculation are integrated, as well as an I2C interface in order to program every coefficient. Extracted layout simulation results demonstrate that the information provided by moment calculation in AMIC helps to improve tridimensional positioning of the detected event. A two-detector test-bench is now being used for AMIC prototype characterization and preliminary results are presented.

KEYWORDS: Analogue electronic circuits; Gamma camera, SPECT, PET PET/CT, coronary CT angiography (CTA); Front-end electronics for detector readout

¹Corresponding author.

Contents

1	Introduction	1
2	Architecture	2
2.1	Input stage	2
2.2	Computational block	2
2.3	Output stage	5
2.4	Digital control	5
3	ASIC characterization	6
4	Experimental setup	7
5	Conclusions	9

1 Introduction

The development of position sensitive detectors such as SiPM arrays and multi anode PMT leads to an increase in their resolution, thus causing a rise in the number of channels to be processed by front-end architectures. While this allows better spatial and energy resolution and provides more information on light distribution, new challenges in front-end design are to be faced in order to process all of this information. As a result, a very active field of research is the design of compact ASIC-based front-ends. The two main approaches are digital and analog data processing. While in digital approach the ASIC front-end usually integrates a pre-amplifier stage, a variable gain amplifier and an analog-to-digital converter (ADC) for each channel [1, 2], analog solutions are generally based on charge integrating circuits and comparators [3, 4]. The main drawback of digital approach is the amount of data that has to be processed by data acquisition (DAQ) stage, since no processing is performed in the front-end. Analog ASICs can be designed in order to pre-process data proceeding from the photo-detectors, thus reducing the number of channels to be digitalized and post-processed.

The aim of our research is to develop a magnetic resonance (MRI)-compatible PET scanner based on continuous scintillator crystals which present better energy resolution [5] when compared to pixellated ones [1]. While front-ends designed for pixellated crystals only perform energy and time measurements, our analog integrated front-end also determines the tridimensional coordinates of the detected event inside the continuous crystal. PESIC (PEt aSIC) was a first prototype based on a charge-division circuit that was presented in [6]. Though benefits in data acquisition were described in [5], the main drawback of the presented ASIC was its closed structure that made expandability impossible without a circuit redesign, so that one of the main goals while designing a

new prototype was to allow expandability of the front-end. As it was presented in [7], light distribution moments analysis can be used to improve front-end performances. Since the whole light distribution is needed, the use of a pixellated scintillator is unfeasible. Furthermore, PESIC was designed for PMT detectors, but since our final aim is to design a MRI-compatible PET scanner, the AMIC prototype features compatibility with SiPM which are immune to magnetic fields.

As a redesign of the integrated front-end was needed, a novel architecture based on light distribution moments analysis is here presented. AMIC is the basic structure of an expandable integrated front-end whose number of input channels can be increased connecting the appropriate number of devices. The limit in total inputs number is given by the noise introduced by each device. The objective of the integrated front-end is to reduce the number of channels that has to be digitalized and post-processed without losing information about the light distribution. Each AMIC can calculate up to 8 programmable moments of a 64-input current distribution, thus providing useful information such as median value, variance, skewness etc. Experimental characterization of AMIC is presented in section 3 and 4, while section 2 focuses on the description of its architecture. Final conclusions and future research are discussed in section 5.

2 Architecture

The final layout and a schematic version are presented in figure 1.

2.1 Input stage

The input stage is composed of 64 current amplifiers. Each of them has to amplify its input current and mirror it into each of the 8 computational blocks. The complexity of the signal path routing between the amplifiers and furthestmost computational blocks requires the introduction of an additional current mirror circuit. As shown in figure 1, 32 amplifiers are located in the upper side of the die, while the remaining 32 are in a symmetrical position at the bottom side of it. In the central part of the die is located a current copy circuit, so that each amplifier directly connects to 4 computational blocks and to the current copy circuit, which then mirrors its input currents into the four remaining computational blocks. Since compatibility with both SiPM and PMT was required, the dominant pole is placed at the input node of the amplifier. This way the high output capacitance of the SiPM does not result in stability problems, even though the bandwidth of the amplifier would be reduced.

The basic architecture of each current amplifier is shown in figure 2. As experiments were to be carried out by using Position Sensitive PMT (PSPMT), in this prototype the input stage is optimized for this kind of detectors. For a typical PSPMT a 34 MHz bandwidth has been measured through simulation. A careful design resulted in a less than 1.4mW per channel power consumption, which is an important issue due to the high number of the integrated input stages. Process mismatches in current copy factor can be compensated by calibrating the coefficients of the computational blocks.

2.2 Computational block

The central core of AMIC is composed of 8 computational blocks, so that 8 different programmable moments of the up to 64 input current distribution can be processed at the same time. Each computational block works as a finite impulse response filter. The programmed moment is calculated

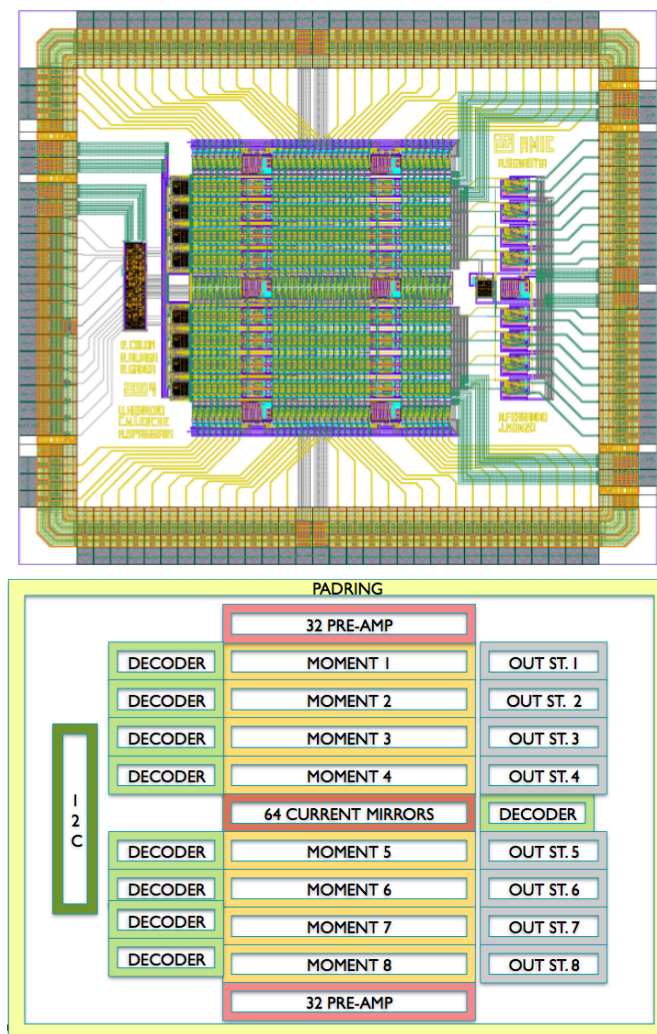


Figure 1. AMIC layout 3.8x3.3 mm (AMS 0.35 μ process).

by multiplying each input current by an appropriate coefficient and summing all of the resulting currents, as shown in figure 3.

Each computational block is composed of 64 coefficient units that work in current mode, so that no current-to-voltage conversion is needed. The coefficient unit is implemented through a linear MOSFET current divider, whose working principle is based on the R-2R ladder that can be found in DAC circuits, as shown in figure 4. Coefficient programmability is achieved by adding a switch at the end of each branch of the ladder, so that only a fraction of the input current reaches the output node. Coefficients are then limited between 0 and 1.

This structure proved to achieve extremely high resolutions, as described in [8]. Since a trade-off between resolution, area, frequency response, and input dynamic range had to be achieved, coefficient units were limited to an 8-bit resolution with no code loss up to 1mA input current and 60MHz bandwidth. The number of effective bits affects the maximum number of the outputs of the detector that can be processed by a front-end based on AMIC devices. For example, the position

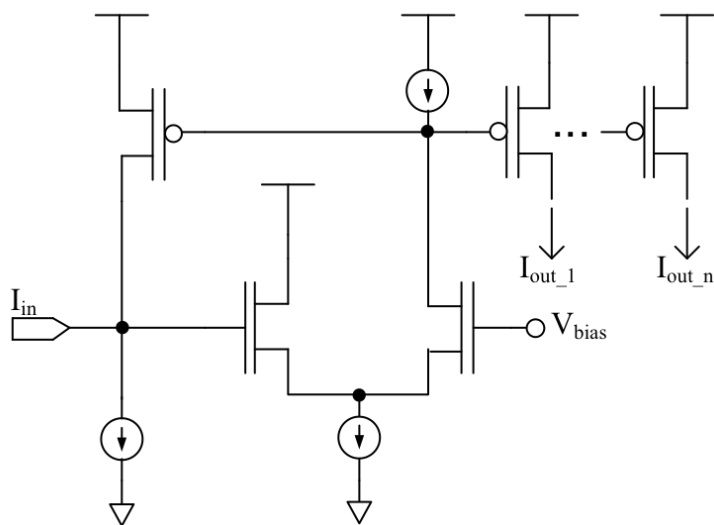


Figure 2. Input stage: current amplifier.

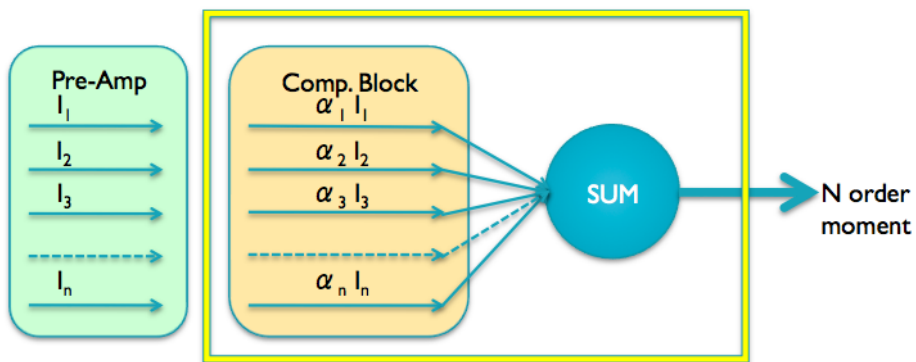


Figure 3. Calculation algorithm for the n-order moment.

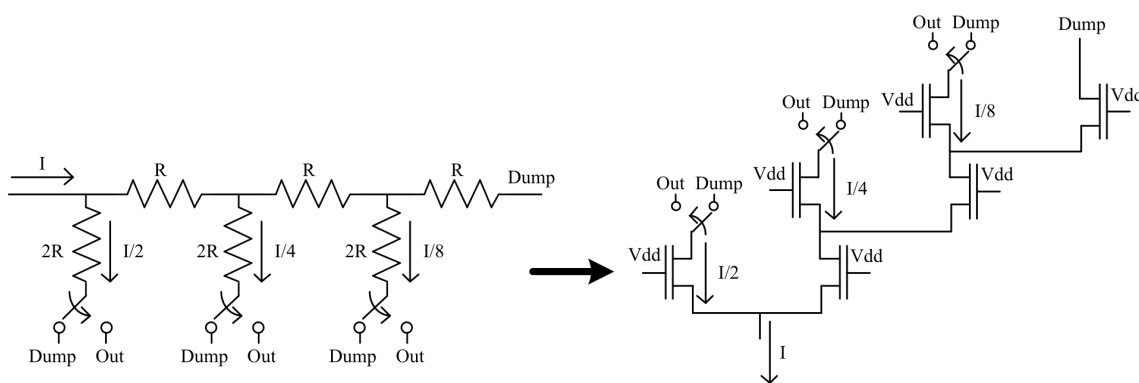


Figure 4. Coefficient unit: working principle and simplified schematic.

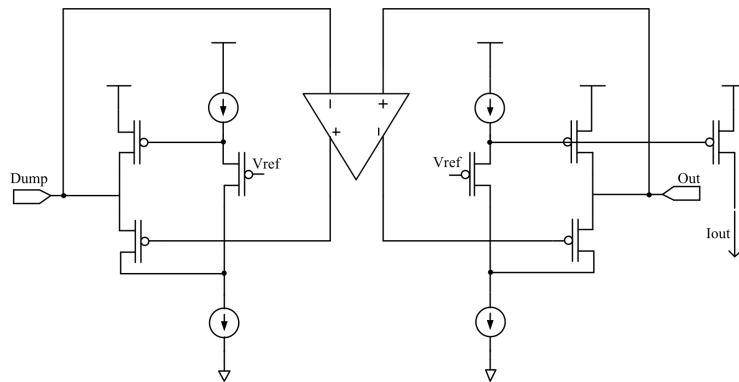


Figure 5. Current collector with fully-differential amplifier.

of an event on the X axis can be obtained with a set of coefficients distributed lineally along the X axis. With 8-bit resolution, 256 values can be resolved. Thus a front-end for a detector of up to 65536 outputs could be developed using AMIC devices. Since the presented architecture proved to be extremely sensitive to voltage variations between Dump and Output nodes, an extremely stable, fully differential current collector was integrated in order to stabilize such nodes and mirror output current into the output stage, as shown in figure 5. Each current collector can handle currents proceeding from up to 16 coefficient units, so that 4 collectors for each computational block are needed. A thoughtful layout design achieved symmetry in the design of the paths in order to decrease voltage variations provoked by parasitic resistances of metal paths. By adding a current collector every 16 coefficients, 4 partial sums between the output currents of the coefficients are performed within each computational block, so that only 4 currents have to be added in the corresponding output stage of each computational block.

2.3 Output stage

One output stage for each computational block is needed to calculate the final current value and to provide two different output signals for each moment. A transconductance amplifier providing a rail-to-rail output voltage for further digitalization and post processing is integrated in each output stage. Furthermore, a current signal for each moment is provided to achieve an expandable structure. Since the algorithm to obtain light distribution moments is purely additive, several AMIC devices can be combined to process the desired number of the output channels of the photodetector.

As shown in figure 6, each AMIC device can calculate up to 8 partial moments of a region of the photodetector. A final stage AMIC is then used to combine the partial moments into the final moments of the whole distribution.

2.4 Digital control

A digital interface based on the I2C standard is integrated and controls the programming of the coefficients. In order to avoid clock noise effects during the analog processing phase, coefficients are locally stored through latches located in the coefficient units. Due to the elevated number of the coefficients, decoders are interposed between the I2C circuit and the storage latches of the coefficients.

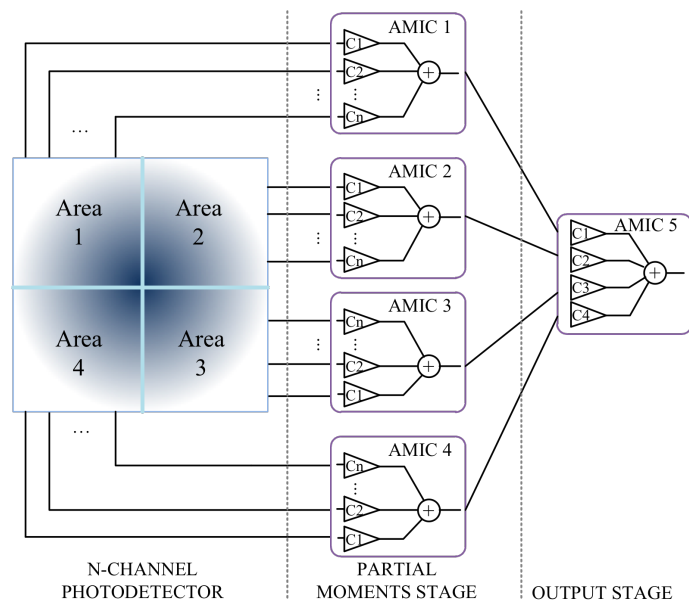


Figure 6. Example of an AMIC-based front-end.

Table 1. Characterization of a typical coefficient unit.

Bandwidth	> 14MHz
Input Dynamic Range	1.65mA
Linearity vs. Input (coeff.value = 128)	$\pm 0.65\%$
THD 0.5mA (100KHz)	0.5%
Noise (Current Output)	$1.8\mu A_{rms}$

3 ASIC characterization

Manufactured prototypes were tested to validate design choices. Since the most important part of AMIC are the computational blocks, a specific test bench was set up to evaluate their performances. Experiments were carried out using a high precision current source and a specifically designed switch matrix array, so that a known amount of current could be injected into a single AMIC input. Several coefficient units were tested. As expected, high input currents approached the linear limit of the coefficient, so that the results here presented refer to this worse case. Results shown in table 1 are those of a typical coefficient.

As can be seen in figure 7, even though most codes are into the $\pm 0.5\text{LSB}$ region, some values present a bigger error, so that the effective achieved bits are 7. This 1-bit loss is due to area constraints in the dimensioning of the coefficient units. Smaller-area transistors are to be integrated in order to achieve the desired amount of coefficients in a reasonable die area, thus increasing sensitivity to process mismatches. As explained in section 2.2, the effective resolution of the coefficients affects the maximum number of the channels of the detectors that could be processed by

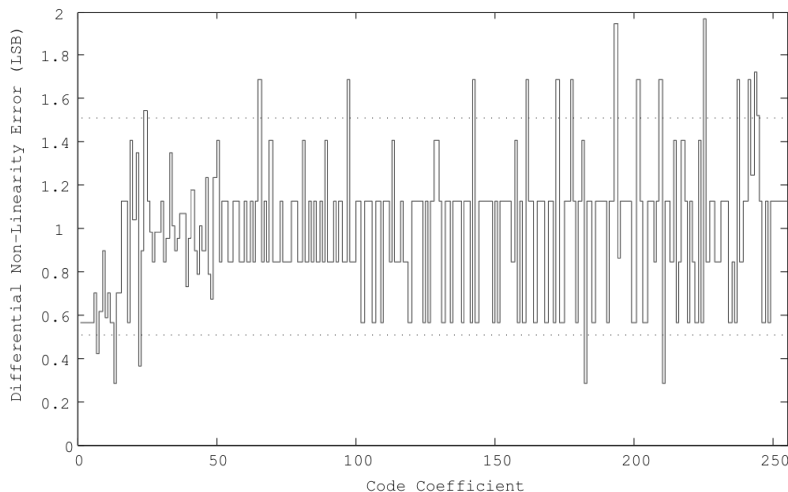


Figure 7. DNL measurements.

an AMIC-based front-end. With 7 effective bits, a maximum of 16384 inputs could be acquired. Experimental tests showed that process mismatches in the pre-amplifier stages cause a difference in the current copy factor, which can be easily compensated by calibrating the values of the coefficients. Finally, tests run on the output stage showed an unexpected noise source, which will lead to a careful redesign in future prototypes. Anyways, the measured noise level is quite negligible compared to the effects of the statistical spread of light distribution.

4 Experimental setup

A two-PET-detector test bench was set up to measure AMIC performances, as shown in figure 8. One detector had been characterized in previous experiments and was used as a reference, while the other mounted an AMIC-based front-end and constituted the device under test (DUT). Both detectors are composed of a 42x42x10mm continuous LSO crystal coupled to a 64-input Hamamatsu H8500 Position Sensitive Photomultiplier Tube, resulting in an original pitch of 5.25mm.

A 0.25mm diameter ^{22}Na gamma source was placed between the two detectors. In order to obtain a 0.5mm diameter spot on the DUT, the reference detector was used to guarantee the appropriate collimation by measuring the diameter of the radiation spot on its surface and adjusting the distance between the source and the DUT. Both the radioactive source and the reference detector were fixed, while the DUT was mounted on high precision engines that could displace it. A 10 by 10 points sweep was carried out on the surface of the detector and a large number of events were acquired at each location. Point spread function was then calculated from experimental data and resolution is given as FWHM. Spatial coordinates were calculated by programming coefficients so as to obtain the first order moment on both X and Y axis. Another set of coefficients was used to measure the energy of the event, so that energy resolution characterization was possible. Finally, a fourth set of coefficients was used to program another computational block so as to calculate the variance of light distribution, which can be used to determine the depth of the interaction (DOI) of the event, as described in [9]. Calibrated coefficients used for X-axis mean value and

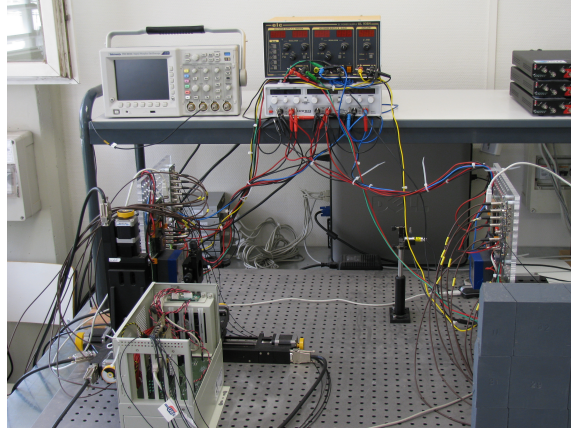


Figure 8. Experimental setup.

Table 2. X axis calibrated coefficients.

37	63	85	112	135	164	191	216
36	61	86	112	140	165	190	217
38	64	89	117	142	171	192	223
37	64	90	112	143	167	196	222
37	63	88	114	141	166	194	220
37	63	88	113	140	165	190	221
37	63	88	116	141	169	192	221
37	63	90	118	142	170	195	223

Table 3. DOI calibrated coefficients.

244	199	172	156	151	172	197	240
193	153	126	115	115	130	157	199
172	126	99	87	86	99	124	172
149	113	87	71	73	85	113	150
145	110	85	72	72	85	110	148
172	131	99	85	85	96	121	172
200	157	131	118	118	130	157	201
241	196	172	160	158	172	201	238

Table 4. Experimental measurements results.

Measure	Mean	St.Dev.	Min.	Max.	Unit
Energy	24.4	7.2	17.1	45.7	%
X centroid	3.86	2.53	1.60	10.19	mm
Y centroid	3.72	2.52	1.50	11.67	mm
DOI	5.07	2.09	1.94	12.08	mm

light distribution variance are shown in table 2 and 3, while the results of the experiments are summarized in table 4.

To better understand the results shown in table 3, a resolution map for surface combined coordinates and another for DOI are shown in figure 9. White points in the bidimensional DOI map have been excluded from calculations due to convergence problems during the fitting process.

Since the detectors are based on a continuous light scintillator, the border effects introduce distortions that degrade resolution as events approach the edges of the detector. Current investigation is centered on evaluating how this resolution loss can be reduced and the performances of the detectors homogenized not only by post processing front-end data, but also by using information

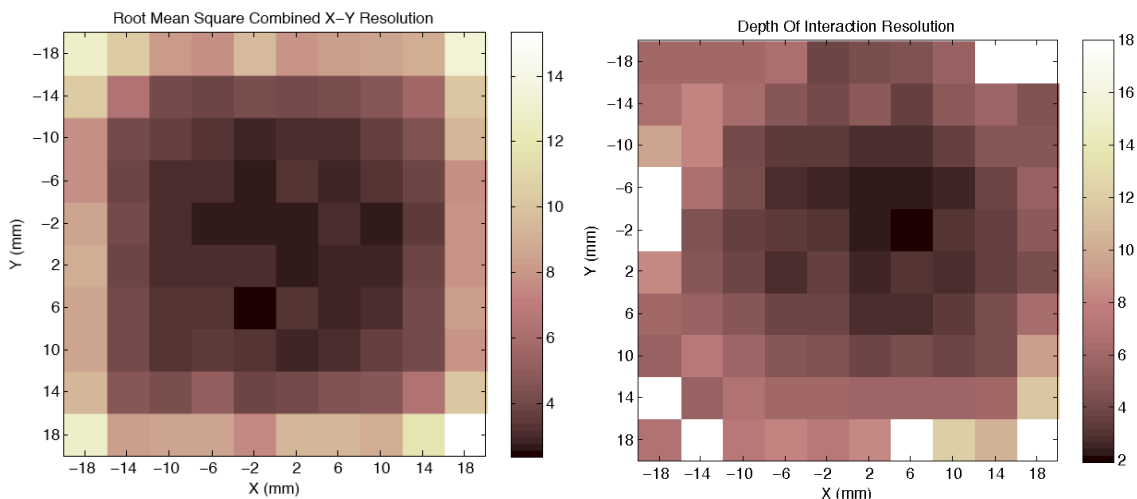


Figure 9. Resolution maps.

provided by higher order moments. As for current results, a spatial resolution mean improvement of over 46% from the original pitch is achieved.

5 Conclusions

Even though no further post processing was applied, experimental results prove that spatial resolution values are similar to those obtained with previous prototypes [6], while DOI measurement is deeply improved and expandability can now be easily achieved by adding more AMIC devices. Furthermore, SiPM compatibility is achieved, which is a key factor in the development of a MRI-compatible PET scanner. Results were obtained using only 4 of the 8 computational blocks integrated in AMIC. More detailed information on light distribution can be obtained by programming the remaining computational blocks of AMIC in order to calculate higher order moments. Finally, post processing algorithms involving the use of artificial neural networks are now being studied in order to integrate all of the information that AMIC can provide and to enhance front-end performances.

References

- [1] Z. Deng et al., *Design of new front-end electronics for animal PET*, *IEEE Nucl. Sci. Symp. Conf. Rec.* **3** (2002) 1543.
- [2] J.Y. Yeom, T. Ishitsu and H. Takahashi, *Development of a waveform sampling front-end ASIC for PET*, in *Proceedings of the 2004 Asia and South Pacific Design Automation Conference*, 27-30 Jan. 2004, pp. 567–568.
- [3] F. Corsi, M. Foresta, C. Marzocca, G. Matarrese and A. Del Guerra, *BASIC: an 8-channel Front-end ASIC for Silicon Photomultiplier Detectors*, *IEEE Nucl. Sci. Symp. Conf. Rec.* (2009) 1082.
- [4] N.A. Mbow et al. *A Full-Custom Mixed-Signal CMOS Front-End Readout Chip for High Efficiency Small Animal PET Imaging*, *IEEE Int. Conf. Electron. Circ. Sys.* (2007) 475.

- [5] V. Herrero et al., *Position sensitive scintillator based detector improvements by means of an integrated front-end*, *Nucl. Instrum. Meth. A* **604** (2009) 77.
- [6] V. Herrero et al., *Pesic: An integrated front-end for PET applications*, *IEEE Trans. Nucl. Sci.* **55** (2008) 27.
- [7] C. Lerche et al., *Fast circuit topology for spatial signal distribution analysis and its application to nuclear medicine imaging*, in *17th IEEE-NPSS Real Time Conference*, May 2010.
- [8] T. Delbruck and P. Lichtsteiner, *Fully programmable bias current generator with 24 bit resolution per bias*, in *Proc. IEEE Int. Symp. Circ. Sys.* (2006) 2852.
- [9] C. Lerche et al., *Depth of interaction detection for γ -ray imaging*, *Nucl. Instrum. Meth. A* **600** (2009) 624.